

## Electronic Supplementary Information (ESI)

### Iron Nanoparticles-Based Supramolecular Hydrogels to Originate Anisotropic Hybrid Materials with Enhanced Mechanical Strength.

Rafael Contreras-Montoya,<sup>a</sup> Ana B. Bonhome-Espinosa,<sup>b</sup> Angel Orte,<sup>c</sup> Delia Miguel,<sup>c</sup> Jose M. Delgado-López,<sup>d</sup> Juan D. G. Duran,<sup>b</sup> Juan M. Cuerva,<sup>a</sup> Modesto T. Lopez-Lopez,<sup>\*b</sup> and Luis Álvarez de Cienfuegos<sup>\*a</sup>

\* Corresponding author email: lac@ugr.es; modesto@ugr.es

- Quantification of Fmoc-FF adsorbed on the MNP@PEG.

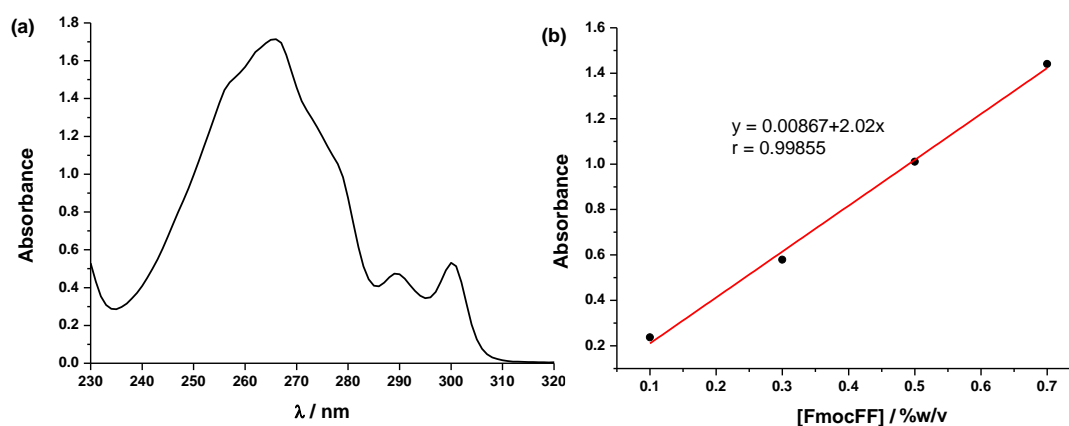


**Figure S1.** a) Absorbance spectra of Fmoc-FF peptide. b) Linear fitting of the absorbance of Fmoc-FF basic solutions of 0.1, 0.3, 0.5 and 0.7% w/v measured at 266 nm.

To quantify the amount of Fmoc-FF adsorbed on the MNP@PEG a calibration line with 0.1, 0.3, 0.5 and 0.7% (w/v) Fmoc-FF basic solutions was performed at 266 nm. The measurements were carried out with diluted samples (200 times) in quartz cuvettes of 1 cm pathlength (Figure S1b). All experiments were repeated 3 times. After measuring the absorbance of the Fmoc-FF supernatant and interpolating in the linear fitting, the result showed that the adsorption of Fmoc-FF on the MNP@PEG was of  $4.7775 \times 10^{-2}$  g Fmoc-FF per gram of MNP@PEG.

- TEM images of FeNPs.

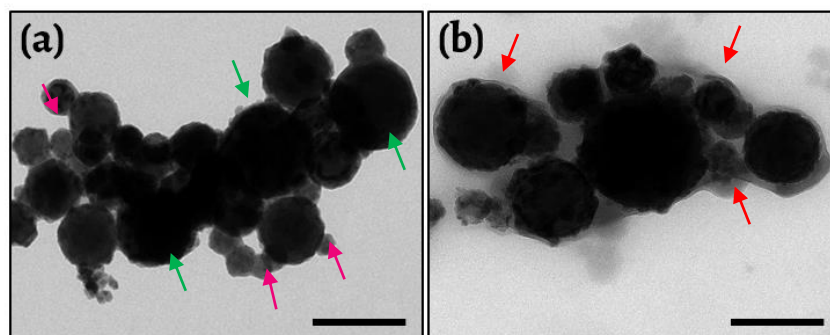


**Figure S2.** TEM pictures of powders of iron nanoparticles (FeNP). (a) Pristine iron nanoparticles; (b) polyethylene glycol (PEG) coated iron nanoparticles. Arrows in part (a) points to smallest and largest nanoparticles; in part (b) to PEG coating. Bar length: 200 nm.

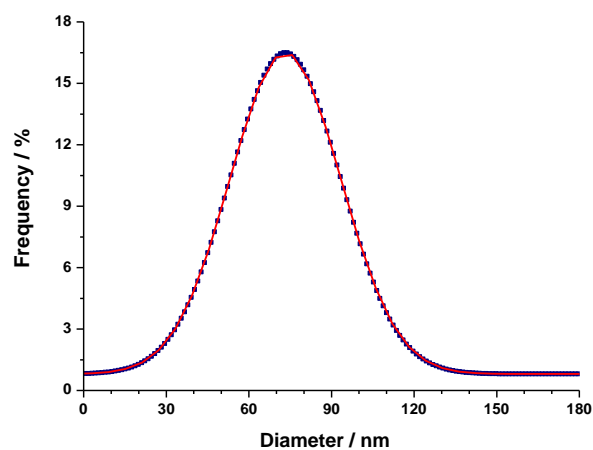


**Figure S3.** Particle size distribution of pristine iron nanoparticles, obtained from pictures like this of Figure S2. Dots represent the experimental data; the continuous (red) line the best fit to a Gaussian distribution function.

- Magnetization studies

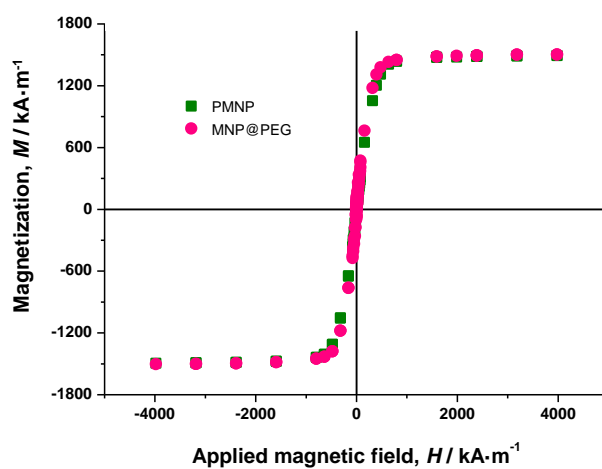


**Figure S4.** Magnetization curves of the iron powders.

Magnetic hydrogel	Concentration of particles according to preparation protocol	$M_{sh}$ (kA/m)	Concentration of particles according to mixing law of magnetims
<b>MHG-0.1</b>	0.1 vol.%	$1.73 \pm 0.09$	$0.111 \pm 0.005$
<b>MHG-0.3</b>	0.3 vol.%	$4.71 \pm 0.24$	$0.307 \pm 0.015$
<b>MHG-0.6</b>	0.6 vol.%	$9.3 \pm 0.5$	$0.61 \pm 0.03$
<b>MHG-0.9</b>	0.9 vol.%	$13.9 \pm 0.7$	$0.91 \pm 0.05$

**Table S1.** Concentration of particles in magnetic hydrogels.

- X-Ray Diffraction (XRD)

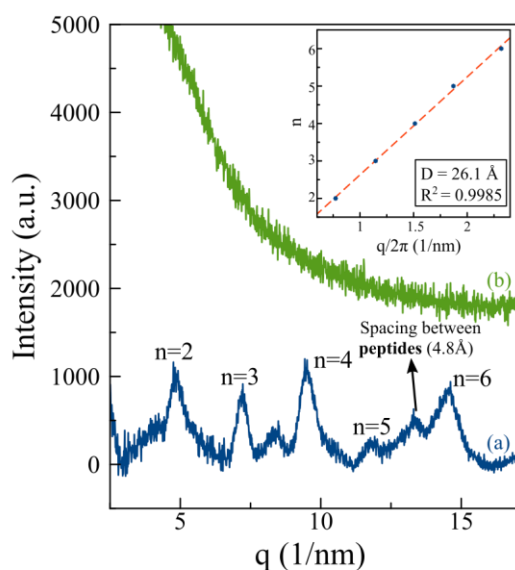


**Figure S5.** X-Ray diffraction patterns of the NMHG (a) and the MHG-0.3 (b). The inset shows the plot of the  $n$ -order of the diffraction peaks as a function of their position (scattering vector,  $q = Q/2 \pi$ ) and the corresponding linear fitting (dotted red line), which provided a fibril width,  $D$ , from the slope of 26.1 Å.

- Rheological characterization

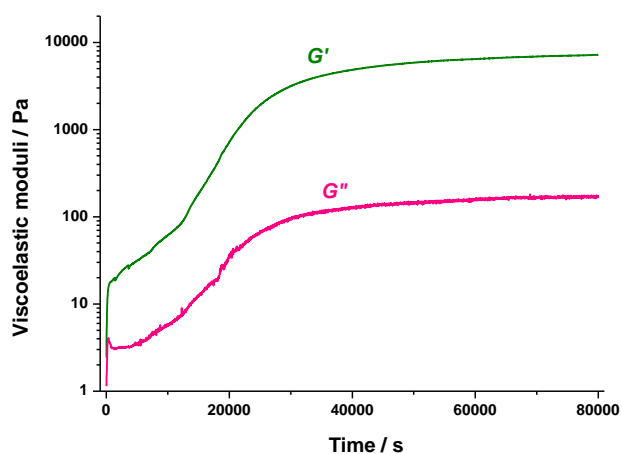


**Figure S6.** Evolution of  $G'$  and  $G''$  for MHG-0.05 hydrogel.

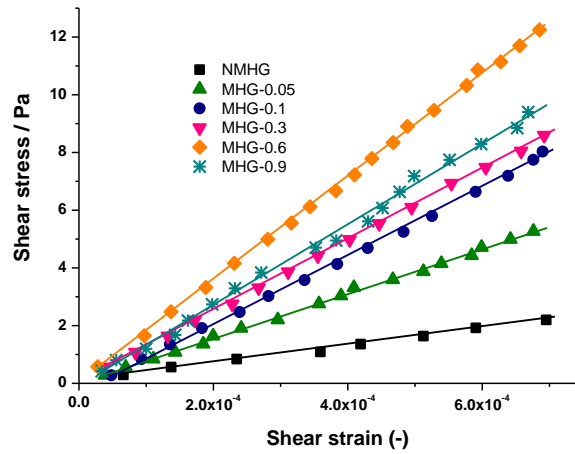


**Figure S7.** Representation of shear stress versus shear strain for magnetic hydrogels.

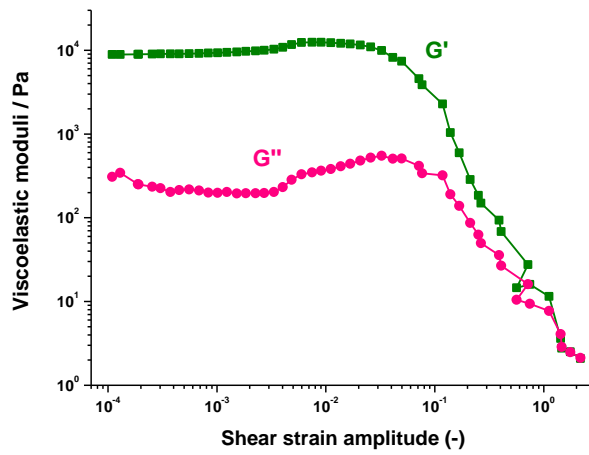


**Figure S8.** Trend of  $G'$  and  $G''$  versus shear strain amplitude for MGH-0.05 hydrogel.

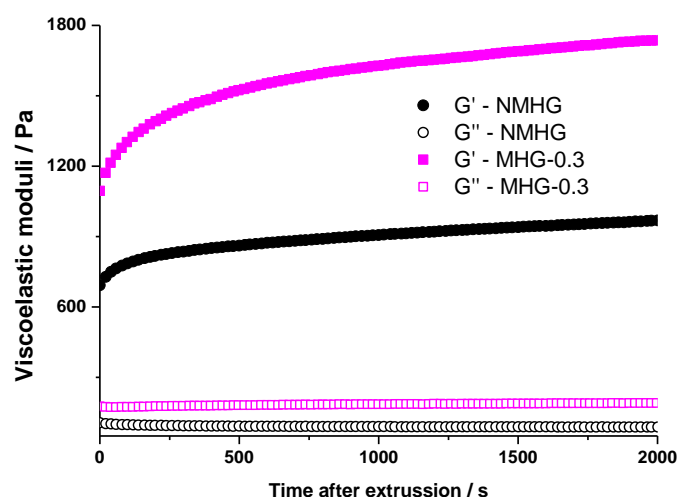


**Figure S9.** Trend of  $G'$  and  $G''$  versus time after extrusion through a 2 mL syringe of 2 mm of gauge.

Accordingly, we selected a measuring system geometry consisting of a parallel plate set of 3.5 cm diameter with serrated surfaces (to avoid wall slip) made of titanium (sensor P35Ti L, Thermo Fisher Scientific, Waltham, MA, USA). We extruded the hydrogels on the bottom plate of the rheometer. Afterwards, we descended the upper plate of the rheometer until perfect contact with the hydrogel was reached, without appreciable compression of the hydrogel. We checked that this condition was satisfied when the normal force reached a value of 0.5 N.

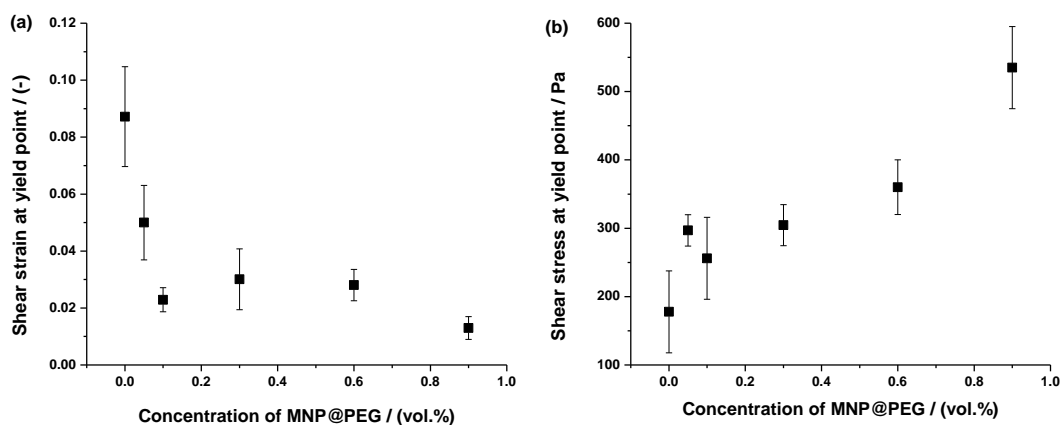


**Figure S10.** (a) Shear strain and (b) shear stress at yield point (maximum in  $G''$  in curves like this of Figure S8) as a function of the concentration of MNP.